JOURNAL OF Materials CHEMISTRY

Characterization of AlSBA-15 prepared by post-synthesis alumination with trimethylaluminium†

Sadanobu Sumiya, Yasunori Oumi, Toshiya Uozumi and Tsuneji Sano*

School of Materials Science, Japan Advanced Institute of Science and Technology, Tatsunokuchi, Ishikawa 923-1292, Japan. E-mail: t-sano@jaist.ac.jp

Received 10th October 2000, Accepted 8th January 2001
First published as an Advance Article on the web 2nd March 2001

The mesoporous siliceous SBA-15 molecular sieve was synthesized and post-synthesis alumination was carried out using trimethylaluminium (TMA). It was found that the aluminium could be easily incorporated into the siliceous framework of SBA-15 without serious structure deformation. From detailed characterization of the prepared aluminium-containing SBA-15 (AlSBA-15) it was also found that it is difficult to keep the aluminium in the framework position after calcination. The hydrothermal stability of SBA-15 was considerably improved by the TMA processing. The results of the cumene cracking reactions and the pyridine adsorption experiments indicated that the Brönsted acid sites of AlSBA-15 are stronger than those of AlMCM-41 prepared by the same method.

1. Introduction

The mesoporous materials MCM-41[1] and FSM-16[2] exhibit a hexagonal array of uniform cylindrical mesopores whose diameters can be systematically varied from 1.5 nm to 10 nm leading to potential applications for the processing of bulky molecules, especially catalysts and absorbents. However, the purely siliceous mesoporous molecular sieves show limited applications because they have poor hydrothermal stability and lack acidity. Therefore, incorporation of various metals, especially aluminium, into the frameworks of mesoporous molecular sieves has been widely studied. In general, aluminium is incorporated into the framework of mesoporous material by a so-called "direct synthesis method"[3–9] in which an aluminium precursor is added into the gel prior to hydrothermal synthesis. The incorporation of aluminium into the framework using the direct synthesis method usually causes a decrease in the structural ordering. Thus, the post-synthesis method,[10–16] which consists of reacting the surface silanol groups on the inner wall surfaces with aluminium chloride or aluminium isopropoxide in nonaqueous solution followed by calcination, has recently been proposed by several researchers. Based on the result of the chemisorption of trimethylaluminium on MCM-41, which was reported by Anwander *et al.*,[17] we investigated the post-synthesis alumination of MCM-41 using trimethylaluminium. It was found that aluminium could be effectively incorporated into the MCM-41 framework without serious structural deformation.[18]

More recently, much effort has been devoted to the incorporation of aluminium into the framework of a newly discovered mesoporous siliceous SBA-15 molecular sieve.[19,20] Besides its large uniform pore size (up to 30 nm), this material has thicker walls than MCM-41, resulting in much higher stability. Incorporation of aluminium into the siliceous framework of SBA-15 by direct synthesis seems unlikely because SBA-15 is synthesized in strong acid media (2 M HCl) and most aluminium sources dissolve under these conditions. From such viewpoints, in this paper we report the post-synthesis alumination of SBA-15 using trimethylaluminium and the detailed characteristics of the prepared AlSBA-15.

†Electronic supplementary information (ESI) available: SAXS patterns and N_2 adsorption–desorption isotherms. See http://www.rsc.org/suppdata/jm/b0/b008168j/

2. Experimental

2.1. Synthesis of SBA-15

Pure siliceous SBA-15 was synthesized according to the literature[19] using the amphiphilic triblock copolymer, poly(ethylene oxide)$_{20}$–poly(propylene oxide)$_{70}$–poly(ethylene oxide)$_{20}$ ($EO_{20}PO_{70}EO_{20}$, average molecular weight 5800, Aldrich). The molar composition of the reaction mixture was 1.00 TEOS : 1.65×10^{-2} $EO_{20}PO_{70}EO_{20}$: 6.95 HCl : 140 H_2O (TEOS = tetraethyl orthosilicate). The synthesis was carried out under various synthesis temperatures and times (see Table 1). The solid product was filtered, washed with deionized water, and dried at 333 K. The SBA-15 prepared was calcined at 823 K for 15 h to decompose $EO_{20}PO_{70}EO_{20}$ and obtain the white powder. This white powder was used as the parent material for post-synthesis alumination of SBA-15.

2.2. Post-synthesis alumination of SBA-15

Prior to alumination with trimethylaluminium (TMA), the synthesized SBA-15 was dried at 553 K for 24 h under vacuum in order to remove adsorbed water as TMA is very water sensitive. 1 g of SBA-15 was dispersed in 10 ml of dry toluene containing various amounts of TMA (1–5 mmol). The resulting mixture was maintained at room temperature for 8 h without stirring. The powder (designated as AlSBA-15) was filtered, washed with dry toluene three times and dried at room temperature under vacuum.

2.3. Characterization

Characterization by Small-Angle X-ray Scattering (SAXS) (MAC Science M18XHF), ^{27}Al MAS NMR (Varian VXP-400), FT-IR (JEOL JIR-7000), N_2 adsorption (Belsorp 28SA) and X-ray fluorescence (Philips PW2400) was carried out to evaluate the efficiency of the alumination with TMA.

Table 1 Surface areas and pore properties for SBA-15 samples prepared under various conditions

Sample no.	Synthesis conditions: Temperature/K	Time/h	Surface area/ $m^2\ g^{-1}$	Pore volume[a]/ $cm^3\ g^{-1}$	Pore diameter[a]/ nm	$d_{(100)}$/ nm
1	308	20	569	0.421	3.64	8.50
2	333	20	726	0.732	5.16	9.43
3	353	20	770	0.811	6.16	9.80
4	363	20	734	0.928	7.06	10.3
5	323	5	598	0.583	4.88	8.77
6	323	10	628	0.612	4.64	8.62
7	323	20	638	0.658	4.64	8.85
8	323	40	630	0.622	4.88	8.85

[a]Determined by the Dollimore–Heal method.

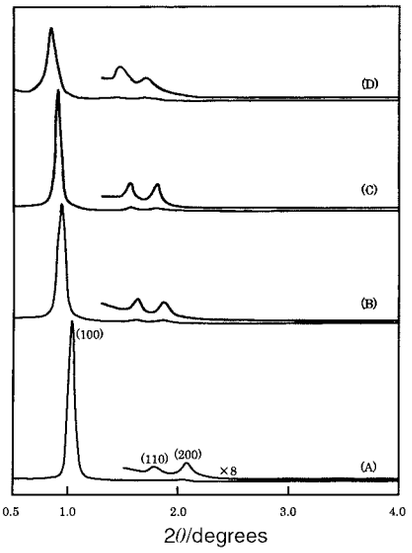

Fig. 1 SAXS patterns of SBA-15 samples synthesized at (A) 308 K, (B) 333 K, (C) 353 K and (D) 363 K.

2.4. Catalytic testing

The cumene cracking was performed in an atmospheric pressure flow system. The AlSBA-15 sample, placed in a quartz tube reactor with a 10 mm inner diameter, was dehydrated at 673 K for 1 h in a nitrogen stream. The temperature was then adjusted to the reaction temperature (523–623 K). The reactant was fed into the catalyst bed with a microfeeder, nitrogen being used as the carrier gas (40 ml min^{-1} flow rate). The contact time (*W*/*F*) was 0.20 h, and the partial pressure of cumene was 7.9 kPa. On-line product analysis was performed on a Shimadzu GC-17A gas chromatograph (FID) with a GL-Science TC-1 capillary column (30 m).

3. Results and discussion

3.1. Synthesis of SBA-15

Synthesis of siliceous SBA-15 as the parent material for the post-synthesis alumination was carried out under varying conditions of synthesis temperature and time. SAXS patterns of the SBA-15 samples are shown in Fig. 1. A well resolved pattern with a prominent peak (100) and two weak peaks (110) and (200) was observed at around $2\theta = 1^\circ$ and 2° which matches well with the pattern reported for SBA-15.[21] The three peaks shifted to lower 2θ with an increase in the synthesis temperature. The SBA-15 sample synthesized at 363 K gave a slightly lower quality SAXS pattern. The synthesis conditions and textural properties of the SBA-15 samples are summarized in Table 1. The pore size distribution and the pore volume were calculated from the desorption branch of the N_2 isotherm by the Dollimore–Heal method. The BET specific surface area, pore volume and pore diameter were strongly dependent upon the synthesis temperature and time. However, after 20 h, the pore volume and pore diameter hardly changed. Judging from the BET surface area and the quality of the SAXS patterns, SBA-15 sample no. 3 was selected for use in the following post-synthesis alumination.

3.2. Alumination of SBA-15

For post-synthesis alumination, the SBA-15 sample was dispersed in dry toluene containing various amounts of TMA. SAXS patterns of the purely siliceous parent SBA-15 and the aluminium-incorporated SBA-15 (AlSBA-15) samples are deposited as ESI.† The SAXS patterns for all AlSBA-15 samples gave one large peak along with two small peaks, characteristic of SBA-15. The intensities of these peaks slightly decreased after alumination, indicating a decrease in the structure ordering. N_2 adsorption–desorption isotherms from purely SBA-15 and AlSBA-15 samples with varying aluminium loadings are deposited as ESI.† Although the amount of N_2 adsorbed decreased slightly with the amount of TMA, sharp inflections in the P/P_0 range from 0.6 to 0.8, characteristic of capillary condensation within uniform pores, were observed. The position of the P/P_0 inflection points is related to a diameter in the mesopore range, and the sharpness of these steps indicates the uniformity of the mesopore size distribution. The calculated BET surface area and pore volume decreased monotonously with the extent of alumination (Table 2). Table 2 also indicates a shift of the (100) peak to higher 2θ values and a lower *d*-spacing for AlSBA-15 with the increased aluminium content. The same phenomenon was observed in the post-synthesis of MCM-41 with TMA.[18] Taking into account that the bond length of Al–O is longer than that of the Si–O bond, it is difficult to explain this result. Shen and Kawi have also observed a shift for the (100) diffraction peak of AlMCM-41 prepared by the direct method and suggested the possibility of distortion of the mesoporous channels of AlMCM-41.[22]

Fig. 2 shows ^{27}Al MAS NMR spectra of the AlSBA-15 samples. The peak intensity was normalized based on 1 g of

Table 2 Characteristics of parent SBA-15 and AlSBA-15 samples prepared by the post-synthesis method with TMA followed by calcination at 773 K for 5 h

Sample no.		Amount of TMA/ mmol	Si/Al[a]	Surface area /$m^2\ g^{-1}$	Pore volume[b]/ $cm^3\ g^{-1}$	Pore diameter[b]/ nm	*d*(100)/ nm	a_0[c]/ nm	Wall thickness[d] /nm
3	SBA-15	—	—	770	0.811	6.16	9.80	11.31	5.15
9	AlSBA-15	1	14.6	613	0.693	6.16	9.52	10.99	4.83
10	AlSBA-15	2	8.4	526	0.654	6.16	9.52	10.99	4.83
11	AlSBA-15	3	5.7	457	0.598	6.16	9.43	10.89	4.73
12	AlSBA-15	4	4.9	432	0.585	5.80	9.43	10.89	5.09
13	AlSBA-15	5	4.8	410	0.564	5.80	9.43	10.89	5.09

[a]The bulk Si/Al was determined by X-ray fluorescence. [b]Determined by the Dollimore–Heal method. [c]Lattice parameter from SAXS data using the formula, $a_0 = 2d(100)/\sqrt{3}$. [d]Pore wall thickness = a_0 − pore diameter.

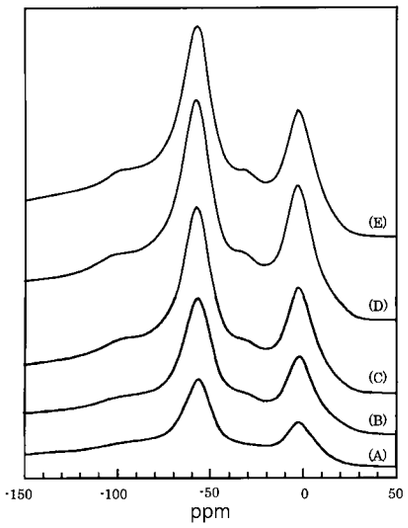

Fig. 2 ^{27}Al MAS NMR spectra of (A) AlSBA-15 (TMA 1 mmol), (B) AlSBA-15 (TMA 2 mmol), (C) AlSBA-15 (TMA 3 mmol), (D) AlSBA-15 (TMA 4 mmol) and (E) AlSBA-15 (TMA 5 mmol).

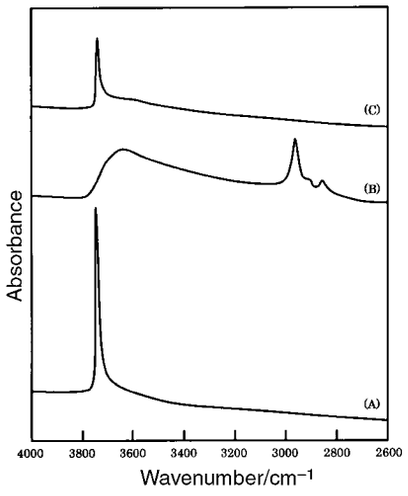

Fig. 3 IR spectra of (A) parent SBA-15, (B) AlSBA-15 before calcination and (C) AlSBA-15 after calcination at 773 K.

sample. All spectra gave two resolved peaks at *ca.* 54 ppm and 0 ppm. The appearance of the peak at *ca.* 54 ppm due to a tetrahedrally coordinated aluminium species means that aluminium atoms have been incorporated into the framework of SBA-15 through the reaction with TMA. The peak at *ca.* 0 ppm is due to an octahedrally coordinated extraframework aluminium species. The result clearly shows the simultaneous presence of both tetrahedrally and octahedrally coordinated aluminium species. The intensities of both peaks increased with the concentration of TMA and reached a constant value at more than 3 mmol of TMA.

IR spectra of the AlSBA-15 prepared by reacting the parent SBA-15 with 3 mmol of TMA are shown in Fig. 3. In the IR spectra of AlSBA-15 before calcination (Fig. 3B), the peak at *ca.* 3740 cm^{-1} assigned to isolated silanol groups was not observed, while the peak at *ca.* 2900 cm^{-1}, assigned to methyl groups of TMA was. The peak at *ca.* 3650 cm^{-1} seems to be due to inaccessible silanol groups in SBA-15.[23] This result indicates that the alumination of SBA-15 takes place through the reaction between TMA and silanol groups on the pore walls. After calcination at 773 K (Fig. 3C), the peak at *ca.* 2900 cm^{-1} disappeared and the peak at *ca.* 3740 cm^{-1} reappeared. The reappearance of the peak at *ca.* 3740 cm^{-1} seems to suggest the formation of silanol groups through the partial dealumination and/or the oxidation of Si–CH_3 surface species[17] during the calcination process.

3.3. Thermal and hydrothermal stabilities of AlSBA-15

At first the thermal stability of AlSBA-15 was studied. The AlSBA-15 sample prepared with 3 mmol of TMA (sample no. 11 in Table 2) was calcined at various temperatures for 5 h. As a reference, SBA-15 sample no. 3 (see Table 2) was also calcined. Table 3 shows the characteristics of the resulting calcined samples. A considerable reduction in the BET surface area and pore volume was observed for both AlSBA-15 and SBA-15 samples calcined at 1073 K and 1173 K. However, the degree of reduction in surface area was slightly smaller for AlSBA-15 than for SBA-15. The inflection due to capillary condensation was clearly observed in the N_2 adsorption isotherm for AlSBA-15 even after calcination at 1173 K.

The hydrothermal stability of AlSBA-15 was also investigated by treatment in boiling water. Fig. 4 shows SAXS patterns for AlSBA-15 (A) and SBA-15 (B) before (a) and after (b–f) the treatment. It is noted that there is a difference in the

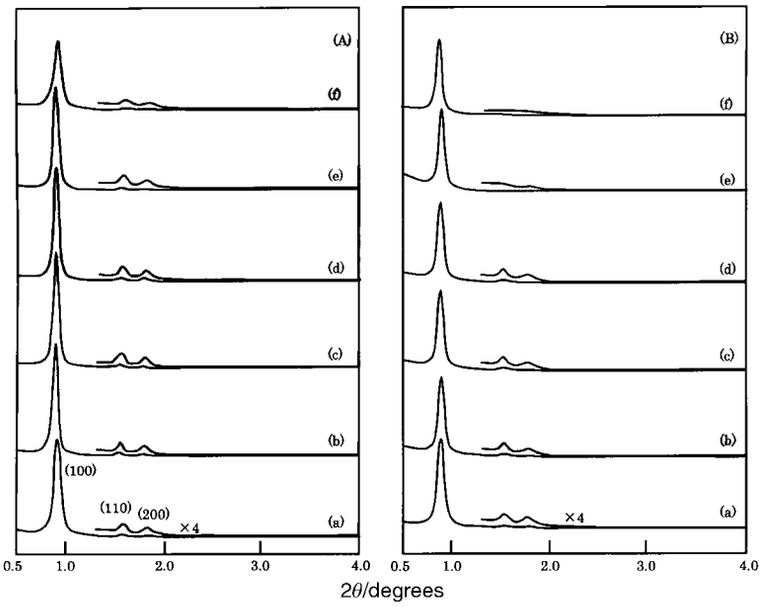

Fig. 4 SAXS patterns of (A) AlSBA-15 and (B) SBA-15 after treatment in boiling water for various times. (a) 0 h, (b) 6 h, (c) 12 h, (d) 24 h, (e) 48 h, (f) 72 h.

Table 3 Characteristics of SBA-15 and AlSBA-15 samples calcined at various temperatures for 5 h

Sample no.		Calcination temperature/K	Surface area/$m^2\ g^{-1}$	Pore volume[a]/$cm^3\ g^{-1}$	Pore diameter[a]/nm
3	SBA-15	873	758	0.851	6.16
3	SBA-15	973	639	0.745	5.80
3	SBA-15	1073	427	0.610	5.46
3	SBA-15	1173	354	0.511	5.16
11	AlSBA-15	773	457	0.598	6.16
11	AlSBA-15	873	448	0.597	6.16
11	AlSBA-15	973	393	0.550	5.80
11	AlSBA-15	1073	345	0.517	5.80
11	AlSBA-15	1173	268	0.420	4.64

[a]Determined by the Dollimore–Heal method.

Table 4 Influence of boiling water treatment on the surface area, pore volume and pore diameter of SBA-15 and AlSBA-15

Sample no.		Treatment time/h	Surface area/$m^2\ g^{-1}$	Pore volume[a]/$cm^3\ g^{-1}$	Pore diameter[a]/nm
3	SBA-15	—	770	0.811	6.16
3	SBA-15	24	410	0.851	7.06
3	SBA-15	48	310	0.759	6.58
11	AlSBA-15	—	457	0.598	6.16
11	AlSBA-15	24	446	0.734	5.46
11	AlSBA-15	48	421	0.662	5.46
11	AlSBA-15	72	406	0.561	5.16

[a]Determined by the Dollimore–Heal method.

peak intensity of the SAXS patterns between SBA-15 and AlSBA-15. The (110) and (200) peaks of SBA-15 mostly disappeared after treatment with boiling water for 48 h. However, the (100), (110) and (200) peaks of AlSBA-15 were clearly observed even after 72 h. Table 4 lists the surface area, pore volume and pore diameter for AlSBA-15 and SBA-15 treated with boiling water for varying periods of time. These results strongly indicate that the hydrothermal stability of SBA-15 is considerably improved by post-synthesis alumination, although a slight reduction in the BET surface area and pore diameter is observed for the AlSBA-15. The enhancement of the hydrothermal stability of MCM-41 by incorporation of aluminium into the framework has been reported in previous studies.[24–26] It is considered that the aluminium-rich surface layer can function as a protective layer for the framework during treatment with boiling water. The same mechanism may be employed to explain the improvement in the hydrothermal stability of SBA-15 after alumination.

3.4. Acidity of AlSBA-15

To evaluate the acidic properties of AlSBA-15 prepared by the post-synthesis alumination of SBA-15 with TMA, IR spectra of pyridine adsorbed on AlSBA-15 (sample no. 11, Si/Al = 5.7) were measured. Fig. 5 shows the IR spectra obtained for pyridine adsorbed on AlSBA-15. As a reference, IR spectra of pyridine adsorbed on the AlMCM-41 (Si/Al = 6.3) prepared by the same procedure (post-alumination with TMA) were also measured. Pyridine vapor (*ca.* 1.3×10^2 Pa) was adsorbed onto the sample at 423 K for 1 h and then IR spectra were recorded at various stages of pyridine desorption, which was continued by evacuation at progressively higher temperatures (423–673 K). Both AlSBA-15 and AlMCM-41 exhibited several peaks due to strong Lewis-bound pyridine (1623 cm^{-1} and 1456 cm^{-1}), weak Lewis-bound pyridine (1577 cm^{-1}) and pyridinium ion on Brönsted acid sites (1546 cm^{-1} and 1641 cm^{-1}) as well as the small peaks due to hydrogen bonded pyridine (1446 cm^{-1} and 1596 cm^{-1}). The peak at 1494 cm^{-1} can be assigned to pyridine associated with both Brönsted and Lewis acid sites. A majority of acid sites generated on both AlSBA-15 and AlMCM-41 are found to be Lewis acid sites. The intensities of these peaks gradually decreased with the evacuation temperature. In the case of AlMCM-41, the peaks due to pyridinium ion on Brönsted acid sites disappeared after evacuation at 623 K. On the other hand, in the case of AlSBA-15, the peaks were still observed even after evacuation at 623 K. Therefore, this strongly suggests that the Brönsted acid sites generated on AlSBA-15 are more acidic than those of AlMCM-41.

3.5. Catalytic activity

The catalytic activity of the prepared AlSBA-15 was also evaluated using the cumene cracking reaction, which requires medium to strong acid sites.[27] The cumene conversions obtained after 30 min on stream at various reaction temperatures are illustrated in Fig. 6. The initial activity of AlSBA-15 was higher than that of AlMCM-41 at every reaction temperature studied. At 523 K, the initial activity of AlSBA-15 was about 10% higher than that of AlMCM-41. The higher activity of AlSBA-15 has also been reported by several other researchers.[9,19] As shown in Fig. 2, both framework and extraframework aluminium species are present in AlSBA-15.

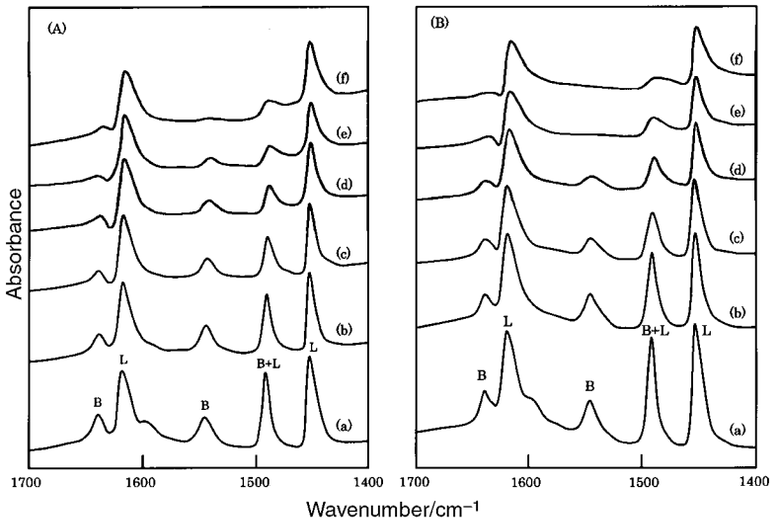

Fig. 5 IR spectra of pyridine adsorbed on (A) AlSBA-15 (Si/Al = 5.7) and (B) AlMCM-41 (Si/Al = 6.3) at various evacuation temperatures. (a) 423 K, (b) 473 K, (c) 523 K, (d) 573 K, (e) 623 K and (f) 673 K. B and L denote Brönsted and Lewis-bound pyridines, respectively.

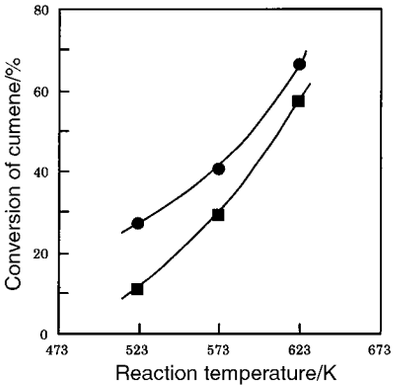

Fig. 6 Initial activity for conversion of cumene at various reaction temperatures on AlSBA-15 (Si/Al = 5.7, ●) and AlMCM-41 (Si/Al = 6.3, ■). Reaction conditions: $W/F = 0.20$ h, N_2 carrier gas flow rate = 40 ml min^{-1}.

To clarify the influence of extraframework aluminium species on the cracking process, the catalytic activity of AlSBA-15 dealuminated at 973 K for 5 h was evaluated. The cumene conversion of the dealuminated AlSBA-15 at 573 K was 11.6%. Taking into account the fact that the peak intensity at *ca.* 54 ppm (due to framework aluminium atoms in the ^{27}Al MAS NMR spectrum of dealuminated AlSBA-15) was approximately 54% of that before the dealumination treatment, this strongly indicates that the cumene cracking reaction takes place on the Brönsted acid sites, *i.e.* the extraframework aluminium species does not influence the cracking process. Therefore, the difference in the cracking activity between AlSBA-15 and AlMCM-41 seems to be attributable to differences in strength of the Brönsted acid sites.

4. Conclusions

Siliceous SBA-15 mesoporous materials were synthesized and impregnated with aluminium to prepare AlSBA-15 by a post-synthesis procedure using TMA. It was found that the aluminium can be easily incorporated into the framework of SBA-15. Characterization of the AlSBA-15 obtained showed that it is difficult to keep the aluminium atoms in the framework positions after calcination. The hydrothermal stability of SBA-15 was improved by post-synthesis alumination. It was also found that the Brönsted acid sites generated on AlSBA-15 are stronger than those of AlMCM-41.

References

1 C. T. Kresge, M. E. Leonowicz, W. J. Roth, J. C. Vartuli and J. S. Beck, *Nature*, 1992, **359**, 710.
2 S. Inagaki, Y. Fukushima and K. Kuroda, *J. Chem. Soc., Chem. Commun.*, 1993, 680.
3 C.-Y. Chen, H.-X. Li and M. E. Davis, *Microporous Mater.*, 1993, **2**, 17.
4 A. Corma, V. Fornes, M. T. Navarro and J. Perez-Pariente, *J. Catal.*, 1994, **148**, 569.
5 Z. Luan, C. Cheng, W. Zhou and J. Klinowski, *J. Phys. Chem.*, 1995, **99**, 1018.
6 H. H. P. Yiu and D. R. Brown, *Catal. Lett.*, 1998, **56**, 57.
7 Z. Zhu, Z. Chang and L. Kevan, *J. Phys. Chem. B*, 1999, **103**, 2680.
8 D. Wei, H. Wang, X. Feng, W. Chueh, P. Ravikovitch, M. Lyubovsky, C. Li, T. Tekeguchi and G. L. Haller, *J. Phys. Chem. B*, 1999, **103**, 2113.
9 Y. Yue, A. Gedeon, J. L. Bonardet, N. Melosh, J. B. D'Espinose and J. Fraissard, *Chem. Commun.*, 1999, 1967.
10 R. Mokaya, W. Jones, Z. Luan, M. D. Alba and J. Klinowski, *Catal. Lett.*, 1996, **37**, 113.
11 R. Mokaya and W. Jones, *Chem. Commun.*, 1997, 2185.
12 R. Ryoo, S. Jun, J. M. Kim and M. J. Kim, *Chem. Commun.*, 1997, 2225.
13 R. Mokaya and W. Jones, *J. Mater. Chem.*, 1999, **9**, 555.
14 M. S. Morey, G. D. Stucky, S. Schwarz and M. Fröba, *J. Phys Chem. B*, 1999, **103**, 2037.
15 W. S. Ahn, D. H. Lee, T. J. Kim, J. H. Kim, G. Seo and R. Ryoo, *Appl. Catal. A*, 1999, **181**, 39.
16 R. Mokaya, *Chem. Commun.*, 2000, 1541.
17 R. Anwander, C. Palm, O. Groeger and G. Engelhardt, *Organometallics*, 1998, **17**, 2027.
18 Y. Oumi, H. Takagi, S. Sumiya, R. Mizuno, T. Uozumi and T. Sano, *Microporous Mesoporous Mater.*, in press.
19 M. Cheng, Z. Wang, K. Sakurai, F. Kumata, T. Saito, T. Komatsu and T. Yashima, *Chem. Lett.*, 1999, 131.
20 Z. Luan, M. Hartmann, D. Zgao, W. Zhou and L. Kevan, *Chem. Mater.*, 1999, **11**, 1621.
21 D. Zhao, J. Feng, Q. Huo, N. Melosh, G. Fredrickson, B. F. Chmelka and G. D. Stucky, *Science*, 1998, **279**, 548.
22 S. C. Shen and S. Kawi, *J. Phys. Chem.*, 1999, **103**, 8870.
23 M. E. Bartram, T. A. Michalske and J. W. Rogers, Jr., *J. Phys. Chem.*, 1991, **95**, 4453.
24 R. Ryoo, J. M. Kim, C. H. Ko and D. H. Shin, *J. Phys. Chem*, 1996, **100**, 17718.
25 L. Y. Chen, S. Jaenikle and G. K. Chuah, *Microporous Mater.*, 1997, **12**, 323.
26 R. Mokaya, *J. Phys. Chem.*, 2000, **104**, 8279.
27 R. Mokaya and W. Jones, *J. Catal.*, 1995, **153**, 76.